

ELECTROANALYSIS

An International Journal Devoted to Electroanalysis, Sensors and Bioelectronic Devices

Voltammetric study of bathocuproine disulphonate/copper system

Journal:	<i>Electroanalysis</i>
Manuscript ID	elan.202400090.R1
Wiley - Manuscript type:	Research Article
Date Submitted by the Author:	12-Apr-2024
Complete List of Authors:	Bura-Nakić, Elvira; Institut Ruder Boskovic Crmarić, Dora; Institut Ruder Boskovic Cukrov, Nuša; Institut Ruder Boskovic Mlakar, Marina; Institut Ruder Boskovic
Suggested Editor:	Manuscripts from Europe (Susana Campuzano Ruiz)
Keywords:	cuprous ion, BCS, reduction mechanism, voltammetry

SCHOLARONE™
Manuscripts

Voltammetric study of bathocuproine disulphonate/copper system

Elvira Bura-Nakić^{1*}, Dora Crmarić¹, Nuša Cukrov, Marina Mlakar¹

¹ Ruđer Bošković Institute, Department for Marine and Environmental Research, Bijenička 54,
10 000 Zagreb, Croatia;

*ebnakic@irb.hr

Summary

The cathodic stripping voltammetry of copper in the presence of a Cu(I) ligand probe (bathocuproine disulfonate - BCS) is investigated. The Cu(I)-BCS and Cu(II)-BCS complexes formed are reduced, at approximately -0.55 V and -0.90 V against Ag/AgCl, respectively. The reduction of Cu(I)-BCS is accompanied by disproportionation to Cu(0) and Cu(II) and Cu(II)-BCS reduction to Cu(0) at potentials of about -0.55 V and -0.90 V vs. Ag/AgCl, respectively. The reduction mechanism of both complexes was recognized as an irreversible redox reaction followed by a chemical dissociation reaction (EC mechanism). The BCS ligand shows strong adsorption on the mercury drop electrode and is a selective ligand for Cu(I) ions, especially when EDTA is added to the solution. By extending the applied accumulation time, adsorptive cathodic stripping voltammetry offers the possibility to study Cu(I) and Cu(II) redox speciation in the nmol concentration range in the environment and in biological matrices.

Keywords: cuprous ion, BCS, reduction mechanism, voltammetry

The reduction of Cu (II) ions in the presence of soft donors is favored, while the preference of Cu(I) for soft donor ligands such as phosphines, thiols, alkenes or alkynes is well known [1]. The complex redox chemistry of copper in the presence of biologically active compounds regulates cellular Cu metabolism [e.g. 2]. However, the observed redox changes make Cu dangerous for the cell, as it is involved in Fenton-like reactions that generate reactive oxygen species (ROS) [2, 3]. The mechanism regulating the cellular homeostasis of Cu is crucial for the prevention of cell damage. The cellular uptake mechanism and redox-related toxicity of Cu are gaining increasing attention from biochemists and environmental chemists.

Enzymatically mediated Cu(II) reduction on the surface of phytoplankton is reported to play an important role in regulating Cu acquisition by various marine algae at low Cu concentrations in oceanic surface waters [4-6]. Walsh et al. (2015) found that cystein (Cys) complexation of Cu(I) increases the bioavailability of Cu to marine phytoplankton through reductive release of Cu(I) from strong Cu(II) ligands. In the same study, a mechanism for the direct uptake of Cu(I)-Cys complexes in *Emiliana huxleyi* is also demonstrated [7].

Equilibrium competition methods, which entangle competition between two ligands for the same metal, are widely used in biology to determine the affinity of metals for protein ligands [8, 9]. In the case of Cu(I) ligand probes with known formation constants used for competitive titrations,

1 they are typically phenanthroline derivatives [8, 9]. One of the phenanthroline derivatives used is
2 the water-soluble bathocuproine disulfonate (BCS), which is highly selective towards Cu(I) and
3 forms a complex of stoichiometry 1:2 [e.g. 9]. Changes in the $(\text{Cu(I)-BCS}_2)^{3-}$ concentration can be
4 monitored spectrophotometrically by following the changes in absorbance at 483 nm. This
5 introduces spectrophotometry as a rapid and relatively affordable method to study Cu(I) affinity
6 to various ligands [9-11].

7 Only a few studies have reported detectable amounts of Cu(I) in rain and fog water, estuaries or
8 ocean waters [12-15]. Although Cu (I) is, at least in an uncomplexed form, thermodynamically un-
9 stable in the presence of oxygen or other oxidants, an appreciable amount of Cu(I) present in the
10 environment is assumed to be a consequence of Cu(II) reduction with sulphite at higher pH values,
11 by reduction with organic compounds, and by various radical and photochemical reactions in the
12 presence of light [12-15]. Nonetheless, speciation models usually assume that only the copper (II)
13 oxidation state is significant. This assumes that the system is at equilibrium and that the pE of
14 seawater is controlled by the $\text{O}_2/\text{H}_2\text{O}$ couple [16-19].

15 Moffet and Zika suggested that a variety of photochemical and thermochemical processes may
16 lead to the formation of Cu(I) in the upper water column [20]. They studied oxidation kinetics of
17 Cu(I) in seawater and concluded that Cu(I) has a sufficiently long lifetime to exist at significant
18 steady-state levels [20]. The same authors measured Cu(I) concentration in surface waters of the
19 subtropical Atlantic, and in the Gulf of Mexico, using selective complexing of Cu(I) with the
20 ligand (2,9 dimethyl-1,10-phenanthroline) and extraction followed by graphite furnace atomic
21 absorption spectroscopy [13]. Depth profiles characteristically displayed surface maxima, where
22 Cu(I) comprised 5 to 10% of the total copper, and a rapid decline with depth. Profiles showed
23 variability with depth and time of day, consistent with the concept of photochemically mediated
24 Cu(II) reduction [13]. However, study of Buerge-Weirich and Sulzberger (2004) on formation and
25 Cu(I) in Estuarine and Marine waters revealed Cu(I) steady state concentrations ranged from 5%
26 to 80% of total dissolved Cu using a solid-phase-extraction based method [14]. Measured Cu(I)
27 was interpreted in the terms of light-induced reduction of Cu(II) and consequent Cu(I) stabilization
28 by chloride at high salinity [14]. Reduction of Cu(II) by sulfide containing compounds at low
29 salinity followed with fast reoxidation of Cu(I) due to stabilization of Cu(II) by strong organic
30 ligands, was assumed at intermediate salinities [14].

31 In this article it was studied electrochemical behavior of BCS and Cu(II)/Cu(I) in the sodium
32 chloride electrolyte using cathodic stripping voltammetry and hanging mercury drop electrode
33 (HMDE). The aim was to explain electrode processes occurring the HMDE surface stabilizing
34 Cu(I) oxidation state in the presence of an selective bidentate hydrophobic ligand (e.g. BCS). This
35 study also provides a basis for future research in the field of environmental electrochemistry and
36 bioelectrochemistry with the aim of developing an electrochemical sensor for the determination of
37 Cu(I) in various samples matrices (e.g. seawater, biological samples) in the low concentration
38 range (nmolar).

2. Experimental

The three-electrode setup was used for measurements using alternating current voltammetry (ACV), cyclic voltammetry (CV), differential pulsed anodic stripping voltammetry (DP-ASV) and square-wave voltammetry (SWV). The reference electrode was Ag/AgCl (3 mol dm⁻³ KCl), the counter electrode was Pt and the working electrode was hanging mercury drop electrode (HMDE). The capacitive current of the double layer formed between an HMDE and electrolyte (aqueous 0.55 mol dm⁻³ NaCl + 0.01 mol dm⁻³ borate buffer) solution containing 0.66 μmol dm⁻³ BCS were recorded by means of phase-sensitive alternating current voltammetry (ACV) using μ-Autolab (Electrochemical Instruments Eco Chemie, The Netherlands) connected to a 663 Stand Metrohm mercury electrode (electrode surface, A=1.68 x 10⁻³ cm²). All other parameters used during ACV and SWV measurements (e.g. deposition potential and time, scan rate, etc.) are given in Figures description in the main manuscript and Supplementary information. All measurements using described three-electrode set up were done under the N₂ atmosphere.

The Cu(I) stock solution was prepared daily by dissolving CuCl in N₂ degassed MQ water containing high concentrations of HCl and NaCl (0.1 and 1 mol dm⁻³, respectively). The Cu(II) standard solution was prepared by dissolving copper(II)-sulfate (CuSO₄; VWR BDH Prolabo Chemicals, Radnor, PA, USA) in MQ water. All supporting electrolyte solutions (0.55 mol dm⁻³ NaClO₄ or 0.55 mol dm⁻³ NaCl) were buffered at pH of ~8.2 by borate buffer with the final concentration of 0.01 mol dm⁻³. Bathocuproine sulfonate disodium salt (BCS) was purchased from Thermo Scientific (purum >97%). Cu(I)Cl salt was supplied from the Alfa Aesar (purum >97%), ortho-Boric acid from VWR, NaOH from LACH NER, NaCl and HCl were supplied from Merck. Total dissolved Cu concentration in Krka River estuary sample was measured by DP-ASV using the standard addition method (*n*=5, supplement Figure 1S). The sample was filtered (0.45 μm pore size, Sartorius) and acidified HNO₃ s.p. to pH < 2 preceding UV digestion for at least 24 hours prior measurements. Each standard addition measurement was performed twice. The voltammograms were processed using the ECDSOFT (ElectroChemical Data SOFTware) software developed in our laboratory (<https://sites.google.com/site/daromasoft/home/ecdssoft>). The peak height was used as the signal value. The parameters used were based on earlier work on DP-ASV measurements of Cu in the estuary [21-24].

3. Results and discussion

3.1. Voltammetry of BCS

On alternating current voltammograms (ACV) capacitive processes of bathocuproine desulfonate (BCS), adsorption and desorption, are recorded at -0.05 and -1.2 V, respectively, without accumulation (Figure 1), while with accumulation third capacitive peak appears which is most probably second layer of BCS molecules adsorbed at the mercury drop electrode surface.

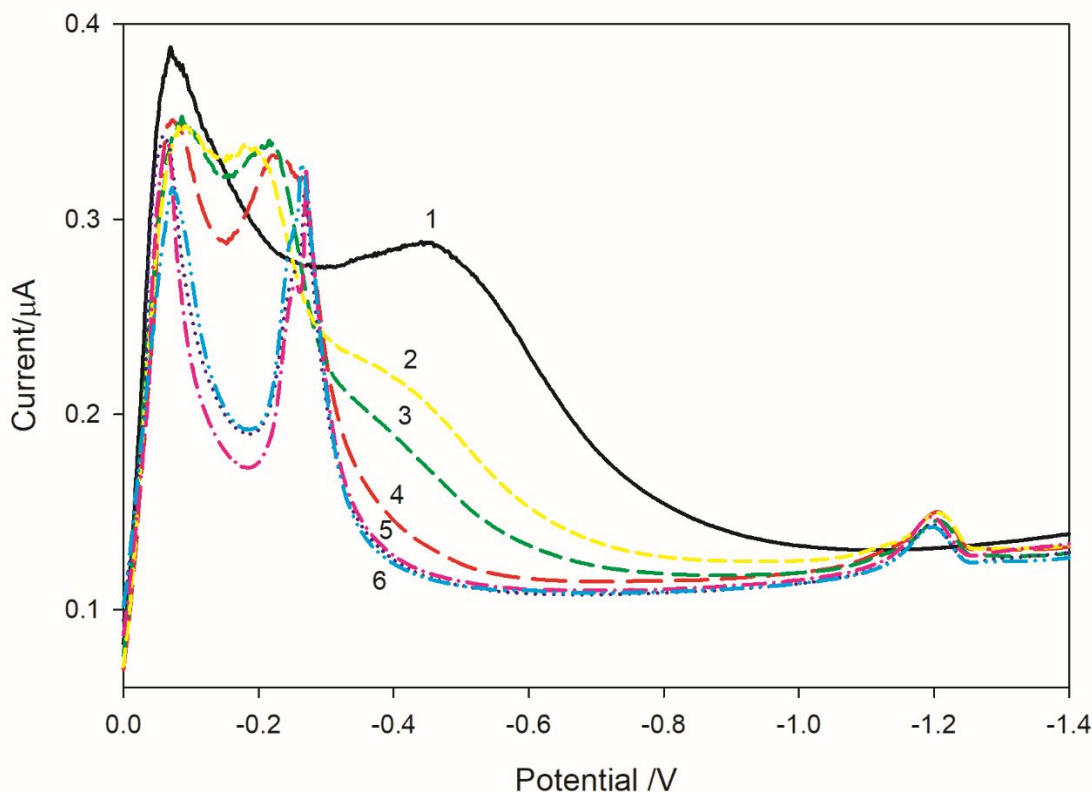


Figure 1 Alternating current voltammetry (ACV, tensometry) ($0.55 \text{ mol dm}^{-3} \text{ NaCl} + 0.01 \text{ mol dm}^{-3} \text{ borate buffer electrolyte solution}$). BCS concentration of $6.6 \times 10^{-7} \text{ mol dm}^{-3}$. Accumulation potential of 0 V ; scan rate 3.2 mV/sec , frequency 75 Hz , phase angle 90° . Accumulation times applied: 1– 0 s ; 2– 15 s ; 3– 30 s ; 4– 60 s ; 5– 120 s ; 6– 300 s .

At square-wave voltammograms (SWV), which is more sensitive to both capacitive and faradic processes, bathocuproine disulfonate (BCS) capacitive peaks, adsorption and desorption, are recorded, as well. Adsorption double peaks appear at about in NaCl at about -0.18 V as response of double layer formed at the mercury drop electrode surface. BCS desorption process takes place in two steps, at -1.14 and -1.30 V . The first peak at -1.14 V corresponds to the desorption of the BCS monomer and the second at -1.30 V to the BCS dimer. Adsorption desorption potentials are very dependent on pH of the NaCl solution (supplement Figure 2S).

3.2 Study of electrochemical behavior of Cu-BCS system

Bathocuproine disulfonate (BCS), preferentially bind Cu(I) over Cu(II) [e.g. 9, 13, 14]. With the addition of BCS ($6.6 \times 10^{-7} \text{ mol dm}^{-3}$) to a chloride solution of Cu(II) at pH 8.2, with different accumulation times at 0.0 V , two reduction peaks were recorded on square-wave voltammograms (Figure 2). Their appearance depends strongly on the BCS concentration, as well as on the accumulation time. Control experiments in which BCS ($6.6 \times 10^{-7} \text{ mol dm}^{-3}$) was added to a buffered chloride solution showed no reduction peaks in the potential range from -0.3 V to -1.0 V

1
2
3 1 on the SWV obtained. The first reduction peak at about -0.55 V appears with lower BCS
4 2 concentrations and shorter accumulation periods, corresponding to the reduction of the Cu(I)-BCS
5 3 complex. As Cu(I) disproportionate to Cu(II) and Cu(0), Cu(II) coordinates with BCS as after
6 4 reduction Cu(I)-BCS, dissociate and only BCS remains adsorbed at the mercury drop surface. It
7 5 reduces at a potential of about -0.9 V. With the BCS excess these reduction peaks decrease and
8 6 adsorption peaks of BCS appear again at the potential about -0.2 V.

11
12 7 Dependence of the Cu(I)-BCS reduction peak height at -0.55 V on the Cu(I):BCS molar ratio,
13 8 confirms the literature reports on the Cu(I)-BCS stoichiometry in the formed complex [8-10]
14 9 (Figure 4S). Namely, at a Cu(I):BCS molar ratio of 0.5 Cu(I)-BCS the reduction peak height
15 10 reaches its maximum, which implies the stoichiometry of the complex Cu(I):BCS = 1:2. Therefore,
16 11 as already confirmed by spectrophotometry the BCS complexes of Cu(II) and Cu(I) both have 2:1
17 12 stoichiometry [8-10, 25].

18
19 13 By increasing the accumulation time the reduction signal of the complex at -0.55 V increase until
20 14 t_{acc} about 120 s with constant reduction potential, while the second one appears with accumulation
21 15 period > 120 s at about -0.9 V and shifts slightly towards negative potentials (Figure 2). The peak
22 16 currents and potentials dependence on the accumulation time for reduction of Cu(I)-BCS at around
23 17 -0.55 V and Cu(II)-BCS at -0.90 V are plotted in Figure 3S. Two reduction peaks were also
24 18 registered on the cyclic voltammograms on the cathode side, at -0.55 V with an accumulation time
25 19 of 60 s (curve 1), while with longer accumulation times (curves 2 and 3) a peak at around -0.90 V
26 20 can be seen, which moves towards negative potentials with the accumulation time (Figure 2, Inset).

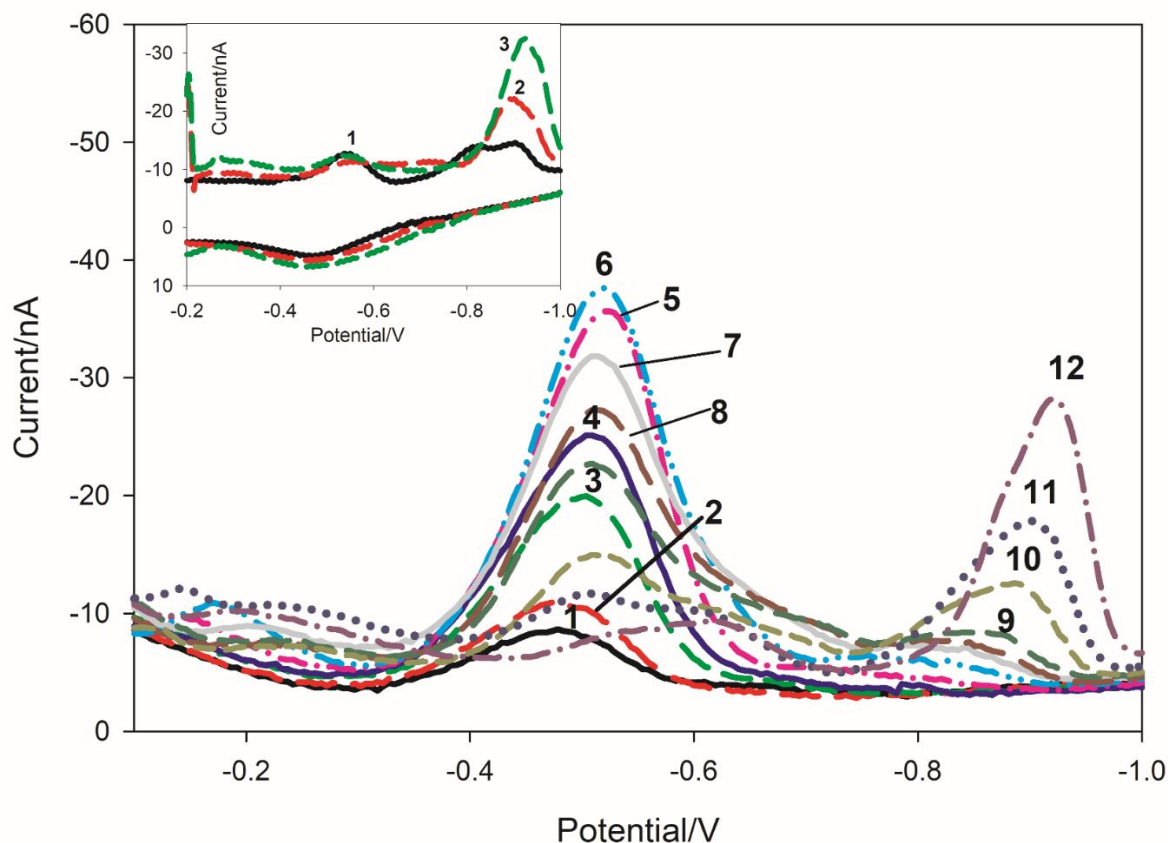


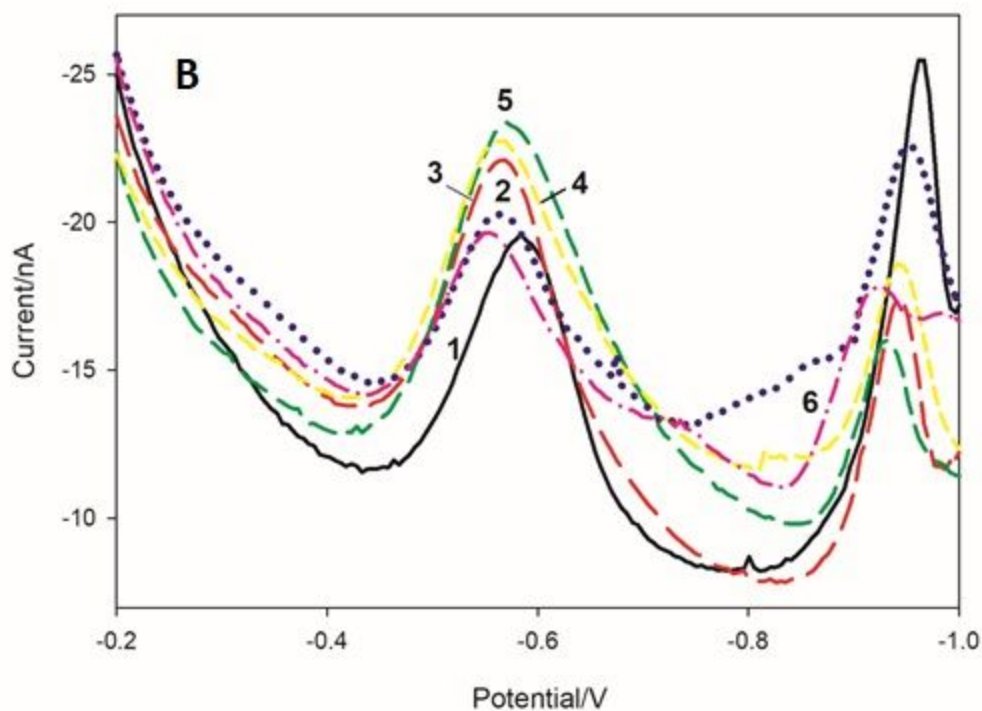
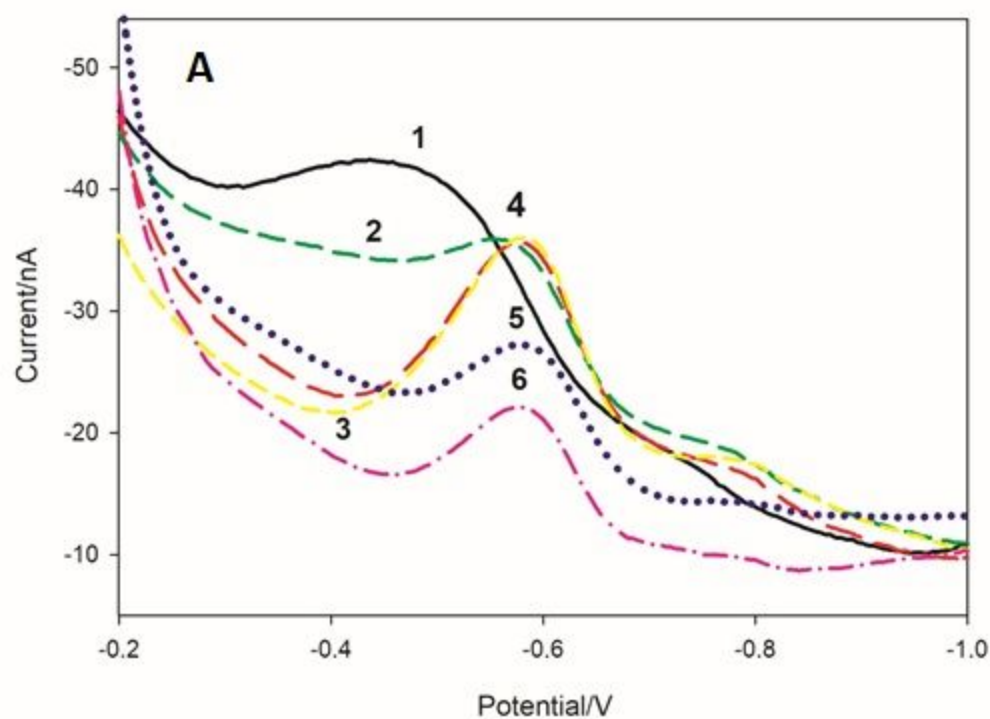
Figure 2 SWV of BCS ($6.6 \times 10^{-7} \text{ mol dm}^{-3}$) and Cu(II) ($4.2 \times 10^{-7} \text{ mol dm}^{-3}$) in sodium chloride electrolyte solution ($0.55 \text{ mol dm}^{-3} \text{ NaCl} + 0.01 \text{ mol dm}^{-3}$ borate buffer) with increasing accumulation time. $E_{\text{acc}} = 0 \text{ V}$; $A = 20 \text{ mV}$, $f = 25 \text{ s}$; t_{acc}/s : 1 – 15; 2 - 20; 3 - 40; 4 - 60; 5 - 90; 6 - 120; 7 - 150; 8 - 180; 9 - 210; 10 - 400; 11 – 600; 12 - 1200. Inset: CV, $v = 50 \text{ mV/s}$; t_{acc}/s : 1 – 60; 2 - 200; 3 – 600.

Square wave voltammetry was used to investigate the dependence of the capacitive BCS processes and the reduction current of the Cu-BCS complexes, as well as the potential, on the pH value in the range from 2 to 9 (Figures 3A and 3B). The concentrations of copper $4.2 \times 10^{-7} \text{ mol dm}^{-3}$ and BCS $6.6 \times 10^{-7} \text{ mol dm}^{-3}$ were kept constant and two accumulation times were used: 45 s and 200 s at 0.0 V, since the second reduction process at -0.9 V only occurs at longer accumulation times. Figure 2S shows the SWV of BCS in the pH range from 2 to 9 after using two accumulation times: 45 s and 200 s at 0.0 V.

It was assumed that the reduction peak at about -0.55 V is the reaction to the reduction of the Cu(I)-BCS₂ complex. After reduction, the complex dissociates and Cu(I) disproportionate to Cu(II) and Cu(0). The reduction peak at about -0.90 V, which is only registered at accumulation times of more than 120 s, corresponds to the Cu(II)-BCS₂ complex reduction to copper amalgam. Various authors provide electrochemical evidence for the formation of the Cu(I) complex as an intermediate stage in the reduction process of various copper(II) complexes with amino acids [26, 27]. Therefore, it can be assumed that the peak at -0.55 V represents the reduction of the Cu(I)-BCS, which is more

1
2
3 1 easily reduced than the Cu(II)-BCS complex. This behavior can be explained by the different
4 2 structures of these two complexes, i.e. Cu(I) prefers a coordination number of two, while Cu(II)
5 3 prefers a coordination number of 4-6, which is regulated by the Jan-Teller effect that is most
6 4 common in octahedral complexes, especially in six-coordinated Cu(II) complexes [28, 29].
7
8
9 5
10
11
12
13
14
15
16
17
18
19
20
21
22
23
24
25
26
27
28
29
30
31
32
33
34
35
36
37
38
39
40
41
42
43
44
45
46
47
48
49
50
51
52
53
54
55
56
57
58
59
60

For Peer Review



1
2
3
4
5
6
7
8
9
10
11
12
13
14
15
16
17
18
19
20
21
22
23
24
25
26
27
28
29
30
31
32
33
34
35
36
37
38
39
40
41
42
43
44
45
46
47
48
49
50
51
52 **Figure 3** SWV of $6.6 \times 10^{-7} \text{ mol dm}^{-3}$ BCS and $4.2 \times 10^{-7} \text{ mol dm}^{-3}$ of Cu(II) in electrolyte solution
53 (0.55 mol dm⁻³ NaCl + 0.01 mol dm⁻³ borate buffer) with increasing pH; deposition potential 0 V;
54 A = 20 mV, f = 25 s; $t_{\text{acc}}/s = 45 \text{ s}$ (A) and 200 s (B). pH: 1 – 6.0; 2 – 6.7; 3 – 7.0; 4 – 7.3; 5 – 8.2;
55 6 – 9.0.
56
57
58
59
60

3.3. Reduction process mechanism

To determine the reduction properties of the complexes, the dependencies of the peak current and the potential on the SW frequency and the SW amplitude were measured [30, 31].

The Cu(I)-BCS reduction current at -0.55 V depends linearly on the SW frequency in the range of (5 - 180) s⁻¹, with a slope of 0.29 ± 0.06 nAs, while Cu(II)-BCS reduction current at -0.9 V linearly on the SW frequency as well, in the range of (5 - 180) s⁻¹, with a slope of 0.26 ± 0.08 nAs [32] (Figure S5). Such behavior is characteristic of irreversible reduction processes. The dependence of the peak potential of the Cu(I)-BCS complex on $\log f$ was linear, with a slope of 7.66 ± 0.17 mV/d.u., while the dependence of the peak potential of the Cu(II)-BCS complex on $\log f$ was also linear, with a slope of 5.88 ± 0.12 mV/d.u. Such behavior is characteristic of the irreversible reduction processes of reactant adsorption. Moreover, after the reduction of the complexes, dissociation takes place, so that we can characterize the reduction processes as an EC mechanism [33].

The peak width at half-height kept on constant with variation of the SWV amplitude confirming irreversible reduction with the reactant adsorption.

Theoretical analysis of the reactant adsorption influence on the SWV of a irreversible redox processes shows that the peak width at half height satisfies the relationship ΔE_p (mV) = $(63.5 \pm 0.5)/\alpha n$ (n is the number of electrons transferred simultaneously and α is the average transfer coefficient [30, 34, 35].

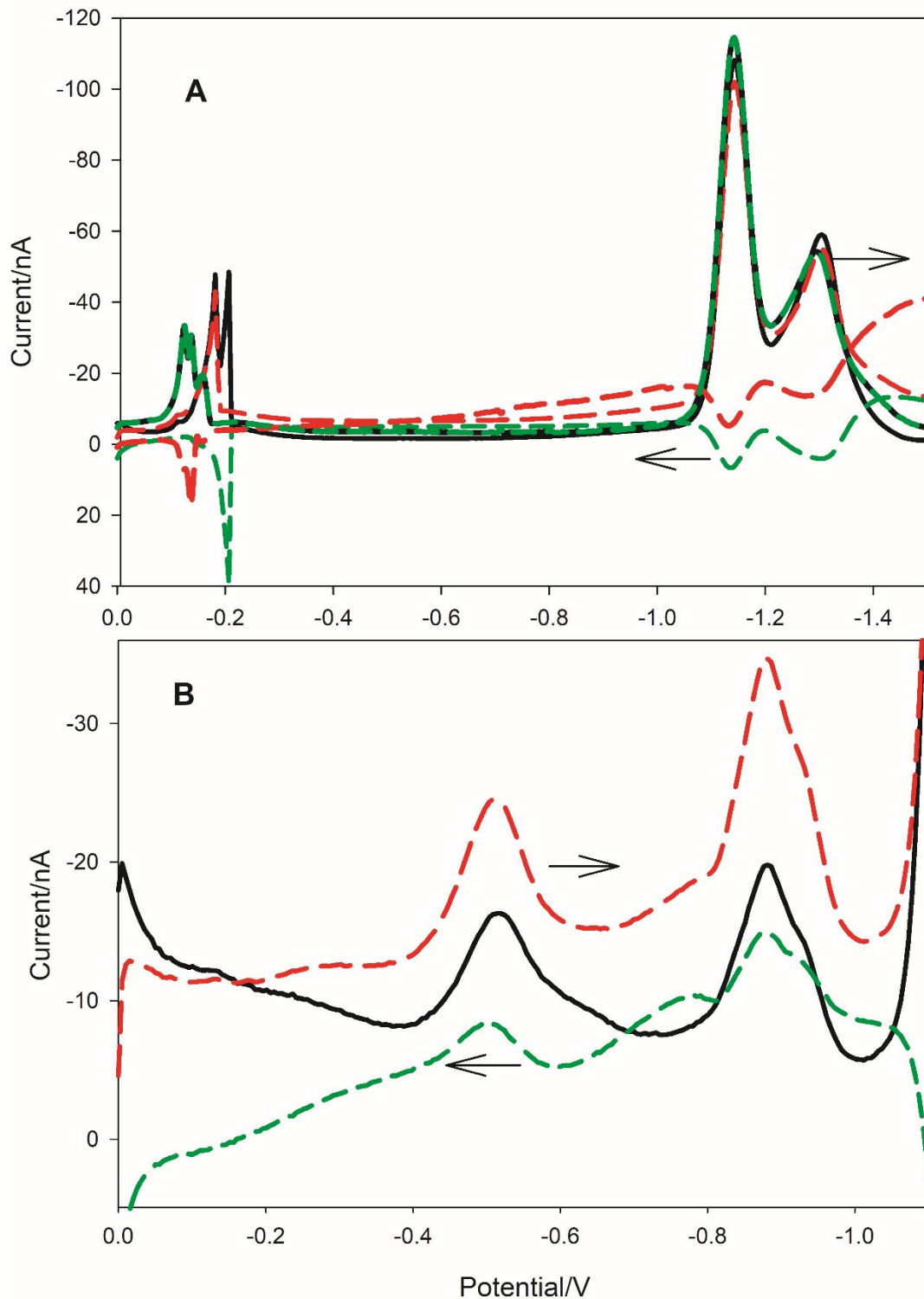
Registered width of the Cu(I)-BCS complex reduction peak at half-height at -0.55 V is 158 mV, which corresponds to a value of $\alpha = 0.40 \pm 0.01$. It is also found that the peak width at half-height remains constant when the SW amplitude changes, which is characteristic of completely irreversible redox processes. Moreover, the reduction peak at around -0.90 V with the width of the reduction peak at half-height is 92 mV, with $\alpha = 0.345 \pm 0.003$, it is assumed that a Cu(II)-BCS complex is formed at the electrode surface with 2 electrons involved in the reduction process. Moreover, both current reduction reactions, Cu(I)-BCS and Cu(II)-BCS, depended linearly on the SW amplitude: Cu(I)-BCS was linear with the slope of $((\Delta i_p/\Delta A)_{A \leq 25}) = (8.32 \pm 0.06) \times 10^{-4} \text{ A V}^{-1}$, while Cu(II)-BCS had the slope of $((\Delta i_p/\Delta A)_{A \leq 25}) = (5.28 \pm 0.43) \times 10^{-3} \text{ A V}^{-1}$ [36] (Figure 5S) According to equation (1):

$$i_p = (5 \pm 1) \times 10^2 q \alpha n^2 F A f \Delta E \Gamma$$

where the amount of adsorbed reactant (Γ) was calculated from the slope $\Delta i_p/\Delta A$ using the values of the transfer coefficients $\alpha = 0.40 \pm 0.01$ and $\alpha = 0.345 \pm 0.003$ of Cu(I)-BCS and Cu(II)-BCS, respectively. n is the number of electrons involved in the reduction processes, $q = 1.68 \times 10^{-3} \text{ cm}^2$ (the surface area of the mercury droplet), $F = 96485 \text{ s A/mol}$ (Faraday constant) and ΔE (square scan increment). The calculated maximum concentration of adsorbed complexes at the electrode surface for the Cu(I)-BCS complex is $\Gamma = 2.69 \pm 10^{-11} \text{ mol cm}^{-2}$, while for the Cu(II)-BCS $\Gamma = 5.29 \pm 10^{-12} \text{ mol cm}^{-2}$.

1
2
3
4 1
5 2 Since the SWV technique distinguishes between Faraday and capacitive current, it provides an
6 3 insight into both half-electrode reactions. The division of the SWV response into forward current,
7 4 measured before the “downward pulse”, and reverse current, measured at the “downward pulse”,
8 5 shows its reduction properties [35, 37]. The variation of SW peak current (i_p) and peak potential
9 6 (E_p) with frequency and amplitude is an important tool to differentiate electrochemical
10 7 mechanisms.

11 8 SWV forward-backward (f-b) scans of BCS capacitive peaks showed two layers at -0.2 V and the
12 9 desorption of BCS monomer and dimer at about -1.15 V and about -1.30 V, respectively (Figure
13 10 4A). The capacitive peaks are reversible, as an adsorption/desorption reaction can be observed in
14 11 the forward-backward scans. The reduction processes of the Cu(I)-BCS (-0.55V) and Cu(II)-BCS
15 12 (-0.90 V) complexes are completely irreversible (Figure 4B) [38, 39].
16
17
18
19
20
21
22
23
24
25
26
27
28
29
30
31
32
33
34
35
36
37
38
39
40
41
42
43
44
45
46
47
48
49
50
51
52
53
54
55
56
57
58
59
60



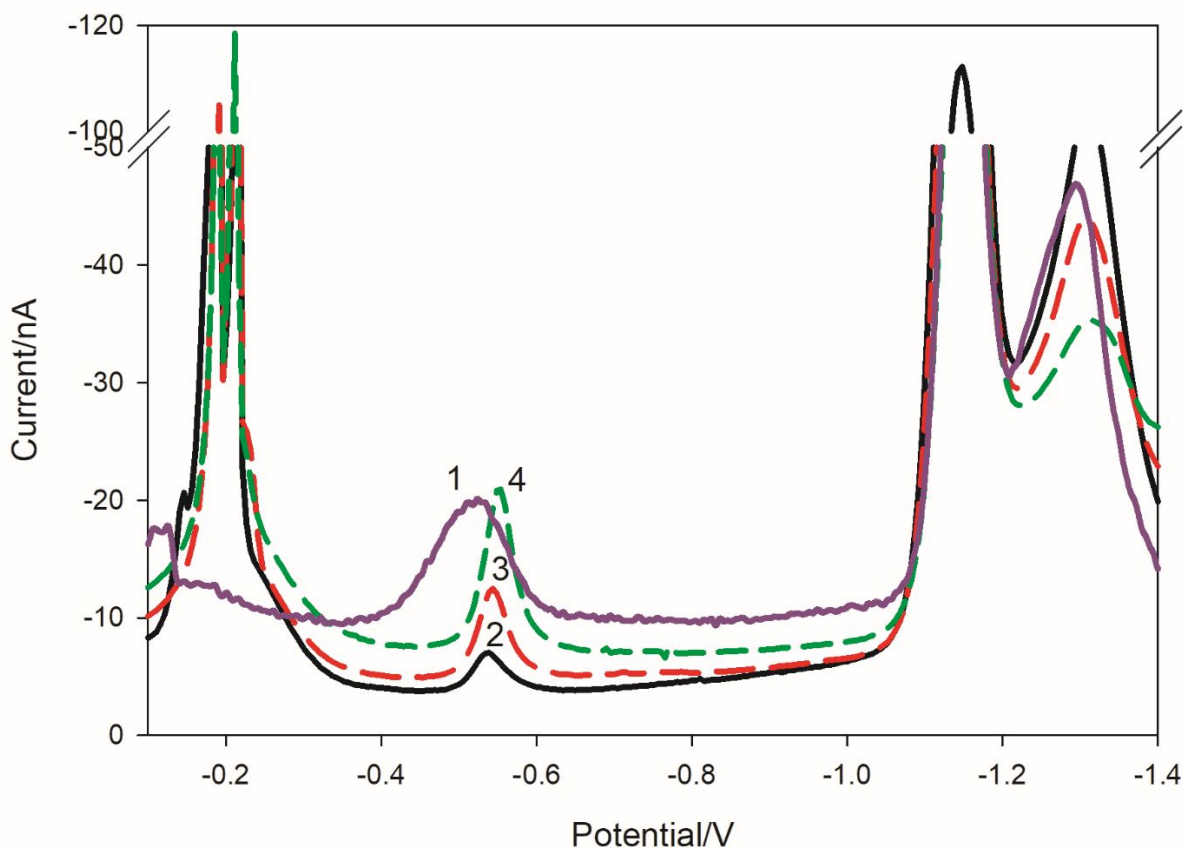
1
2
3
4
5
6

Figure 4 SW backward-forward voltammograms of the BCS (A) and Cu(I)-BCS and Cu(II)-BCS complexes (B). Conditions $6.6 \times 10^{-7} \text{ mol dm}^{-3}$ BCS and $4.2 \times 10^{-7} \text{ mol dm}^{-3}$ of Cu(II), pH = 8.2; $a = 20 \text{ mV}$; $f = 25 \text{ s}^{-1}$; $t_{\text{acc}} = 200 \text{ s V}$ vs. Ag/AgCl.

3.4 Selectivity of BCS towards Cu(I)

The aim of this work was to test the applicability of the method already described in the literature for the selective determination of Cu(I) in natural samples using an electroanalytical method and an Hg electrode as a working electrode [13, 14]. Methods for measuring Cu(I) usually consist of complexing Cu(I) with bathocuproine (BCP) or its disodium salt (bathocuproine disulfonic acid disodium salt, BCS) or complexing Cu(I) with neocuproine, while Cu(II) interference is inhibited by masking ligands such as ethylenediamine, ethylenediamine tetraacetic salt (EDTA) or diethylenetriamine pentaacetate (DTPA) [13, 14, 20, 40]. The BCS forms complexes with both Cu(I) and Cu(II) with a $\log \beta_{\text{Cu(I)BCS}_2}$ of 19.8 and a $\log \beta_{\text{Cu(II)BCS}_2}$ of 11.9, respectively. The addition of EDTA masks Cu(II) present, as $\log \beta_{\text{Cu(II)EDTA}_2}$ is much higher (around 18) than $\log \beta_{\text{Cu(II)BCS}_2}$ [9, 41]. Subsequently, the Cu(I) concentration is determined either by spectrophotometry or liquid-liquid solid-phase extraction with atomic absorption spectroscopy. Here, the solid phase extraction (SPE) method was adapted to detect the Cu(I) occurrence in the Krka river estuary [14]. To increase the selectivity of BCS over Cu(I), the mixture of EDTA/BCS was prepared following the work of Moffet and Zika and Buerge-Weirich and Sulzberger [13, 14], as EDTA is able to remove potential Cu(II) interferences in biological and estuarine/seawater matrices [13, 14, 29] (Figure 6S). An EDTA/BCS mixture with a 5-fold excess of EDTA over BCS, was added to the electrolyte solution containing 0.55 mol dm^{-3} NaCl and 0.01 mol dm^{-3} borate buffer. After the addition of Cu(II), an accumulation step was performed at 0.0 V and the reduction peak of Cu(I)-BCS₂ was not visible in the obtained SW voltammogram, even at longer accumulation times (up to 300 s or more), confirming the selectivity of BCS over Cu(I) in the presence of EDTA. In contrast, when Cu(I) was added in such an electrolyte, the reduction peak characteristic of the Cu(I)-BCS complex was observed at about -0.55 V. The methodology described in this manuscript is satisfactory for Cu(I) determination in coastal and estuarine waters where high concentrations of total dissolved copper are observed [14, 42]. In an estuarine sample, the total copper concentration was determined after UV sample pretreatment using the standard addition method and was found to be $(2.25 \pm 0.5) \times 10^{-7} \text{ mol dm}^{-3}$. To test the applicability of our method for the determination of Cu(I) with the Hg electrode, we added a mixture of BCS/EDTA (molar ratio 1:5) to the filtered sample (0.45 μm filter pore size), in which a high total amount of dissolved Cu was already measured. In the SW voltammogram obtained (Figure 5), when the BCS/EDTA mixture was added to the estuary sample, the reduction peak at around -0.55 V (vs. Ag/AgCl) was already detected after 60 s of accumulation, indicating high Cu(I) contents in the sample under investigation. The result is consistent with the work of Buerge-Weirich and Sulzberger [14], who found high Cu(I) contents in the Scheldt estuary and the North Sea, and with the work of Whitby et al. who predicted that up to 90% of the total dissolved copper in the salt marsh estuary is in the form of Cu(I) [14, 43]. All this suggests that there is a need to develop instrumentation for redox speciation of copper in the nmol concentration range in the difficult seawater matrix, where electroanalytical methods and the hydrophobic Hg electrode surface are advantageous. Although the concentration of total dissolved copper was high due to its proximity to the marina, we believe that the methodology presented

1 here can also be applied to study copper redox cycling and at lower concentrations of total
2 dissolved copper [42].



3
4 **Figure 5** SW voltammograms of natural seawater sample, t_{acc}/s : (1) 60; (2) 120; (3) 300; (4) 600;
5 $E_{\text{acc}} = 0.0 \text{ V}$; $A = 25 \text{ mV}$, $f = 25 \text{ s}^{-1}$. $[\text{BCS}/\text{EDTA}] = 0.66 \times 10^{-7} \text{ mol dm}^{-3} / 3.33 \times 10^{-6} \text{ mol dm}^{-3}$.

7 Conclusions

8 Our study shows that the Hg electrode surface can potentially be used for the investigation of Cu
9 redox speciation in biological and environmental samples. Chemical reaction at the mercury drop
10 electrode (EC) mechanism is described and it is clear that after reduction process of both
11 complexes' dissociation takes place, considering that redox process is characterized as totally
12 irreversible by SWV and CV (EC mechanism). Furthermore, after the reduction of Cu(I)-BCS,
13 copper(I) disproportionate into Cu(0) and Cu(II) in the chloride solution and Cu(II) binds to BCS,
14 whose reduction takes place at a potential of around -0.9 V. The fivefold excess of EDTA over
15 BCS ensures the selectivity of the BCS ligand over the Cu(I) oxidation state. In addition, by
16 extending the applied accumulation time, the Hg electrode and adsorptive cathodic stripping
17 voltammetry offer the possibility to study Cu(I) vs. Cu(II) redox speciation in the nmol
18 concentration range. Voltammetry also appears to be a promising tool for studying the interaction

1
2
3 1 of Cu(I) with biologically important compounds such as amino acids, and competitive equilibrium
4 2 titrations against BCS offer a cost-effective alternative to colorimetric determination of Cu(I)
5 3 ligand affinity.
6 4
7 5
8 6
9 7
10 8

14 9 **Acknowledgments**

15 10
16 11 This research is supported by the Croatian Science Foundation and Swiss National Science
17 12 Foundation project IPCH-2020-10-4965: “Understanding copper speciation and redox
18 13 transformations in seawater”.
19
20
21
22
23
24
25
26
27
28
29
30
31
32
33
34
35
36
37
38
39
40
41
42
43
44
45
46
47
48
49
50
51
52
53
54
55
56
57
58
59
60

References

- [1] B.J. Hathaway 1987, In *Comprehensive coordination chemistry* (eds) G Wilkinson, R. D. Gillard and J. A. McCleverty (Oxford: Pergamon) vol. 5, p. 534.
- [2] C. Y.-S. Chung, J. M. Posimo, S. Lee, C. J. Chang. *PNAS* **2019**, 116, 18285–18294
- [3] N. Sanghai, G. K. Tranmer. *Antioxidants* **2022**, 11, 52.
- [4] L. Kong, N. M. Price. *Limnol. Oceanogr.* **2010**, 65, 601–611.
- [5] H. Whitby, A. M. Posacka, M. T. Maldonado, C. M. G. van den Berg. *Mar. Chem.* **2018**, 204 36–48.
- [6] S. H. Little, D. Vance, M. Siddall, E. Gasson. *Global Biogeochem. Cycles* **2013**, 27, 780–791.
- [7] M. J. Walsh, S. D. Goodnow, G. E. Vezeau, L. V. Richter, B. A. Ahner. *Environ. Sci. Technol.* **2015**, 49(20), 12145–12152.
- [8] Z. Xiao, J. Brose, S. Schimo, S. M. Ackland, S. La Fontaine, A. G. Wedd. *J. Biol. Chem.* **2011**, 286, 11047–11055.
- [9] Z. Xiao, A. G. Wedd. *Nat. Prod. Rep.* **2010**, 27, 768–789.
- [10] J. T. Rubino, M. P. Chenkin, M. Keller, P. Riggs-Gelasco, K. J. Franz. *Metallomics* **2011**, 61–73.
- [11] M. D. Page, J. Kropat, P. P. Hamel, S. S. Merchant. *Plant Cell* **2009**, 21, 928–943.
- [12] H. Xue, M. L. S. Concalves, M. Reutlinger, L. Sigg, W. Stumm. *Environ. Sci. Technol.* **1991**, 1716-1722.
- [13] J. W. Moffett, R. G. Zika. *Geochim. et Cosmochim. Acta* **1988**, 52, 1849–1857.
- [14] D. Buerge-Weirich, B. Sulzberger. *Environ. Sci. Technol.* **2004**, 38, 1843-1848.
- [15] R.J. Kieber, S. A. Skrabal, C. Smith, J. D. Wiley. *Environ. Sci. Technol.* 2004, 38, 3587–3594.
- [16] A. Zirino, S. Yamamoto. *Limnol. and Oceanogr.* **1972**, 17, 661–671.

- 1
2
3
4 1
5 2 [17] D. Dyrssen, M. Wedborg in *The Sea: Equilibrium calculations of the speciation of elements*
6 3 in seawater, vol. 5 (Ed. E. D. Goldberg), Wiley Intersciantia, New York, **1974**, pp. 181–195.
7 4
8 5 [18] W. Stumm, J. J Morgan *Aq. Chem.* 2nd ed., John Wiley & Sons Ltd, New York, **1981**.
9 6
10 7 [19] R. W. Zuehlke, D. R. Kester in *Trace metals in sea water*, vol. 9 (Eds.: C. S. Wong, E. Boyle,
11 8 K. W. Bruland, J. D. Burton, E. D. Goldberg), NATO Conference Series, Springer, Boston, MA.
12 9 **1981**, pp. 773–788.
13 10
14 11 [20] J. W. Moffett, R. G. Zika, *Mar. Chem.* **1983**, 11, 239–251.
15 12
16 13 [21] A. - M. Cindrić. *Distribution, speciation and fate of trace metals in the stratified Krka river*
17 14 *estuary* [PhD thesis]. Faculty of Science, **2015**.
18 15
19 16 [22] D. Omanović, Ž. Kwokal, A. Goodwin, A. Lawrence, C. E. Banks, R. G. Compton, Š.
20 17 Komorsky-Lovrić. *Journal of the Iranian Chemical Society*, **2006**, 3, 128–139.
21 18
22 19 [23] S. Marcinek. *Multimethodological study of trace metal speciation and organic matter in*
23 20 *estuarine waters*. Faculty of Science, **2021**.
24 21
25 22 [24] Y. Louis, C. Garnier, V. Lenoble, S. Mounier, N. Cukrov, D. Omanović, I, Pižeta. *Mar. Chem.*
26 23 **2006**, 114, 110–119.
27 24
28 25 [25] D. Chen, N. Darabedian, Z. Li, T. Kai, D. Jiang, F. Zhou. *Anal. Biochem.* **2016**, 497, 27–35.
29 26
30 27 [26] P. S. Zacharias, T. Sreenivas, J. M. Elizabathe. *Polyhedron* **1986**, 5, 1383–1386.
31 28
32 29 [27] I. Čuljak, M. Mlakar, M. Branica. *Electroanalysis* **1995**, 7, 64–69.
33 30
34 31 [28] M. M. Correia dos Santos, M. L. Simões Gonçalves. *Electroanalysis* **1991**, 3, 131–138.
35 32
36 33 [29] J. Chaboy, A. Muñoz-Páez, P.J. Merkling, E. Sánchez Marcos. *The J. of Chem. phys.* **2006**,
37 34 124, 064509.
38 35
39 36 [30] M. Lovrić, Š. Komorsky-Lovrić, R.W. Murray. *Electrochim. Acta* **1988**, 33(6), 739–744.
40 37
41 38 [31] A. Bačinić, S. Frka, M. Mlakar. *Bioelectrochem.* **2022**, 144, 108009.
42 39
43 40 [32] M. Lovrić, Š. Komorsky-Lovrić. *Int. J. of Electrochem.* **2012**, 596268.
44 41
45 42
46 43
47 44
48 45
49 46
50 47
51 48
52 49
53 50
54 51
55 52
56 53
57 54
58 55
59 56
60 57

- 1
2
3 1
4 2
5 3
6 [33] V. Mirčeski, R. Gulaboski, M. Lovrić, I. Bogeski, R. Kappl, M. Hoth. *Electroanalysis* **2013**,
7 4 25, 2411–2422.
8 5
9 6
10 [34] Š. Komorsky-Lovrić, M. Lovrić. *Fresenius' J. Anal. Chem.* **1989**, 335, 289–294.
11 7
12 [35] A. Bačinić, L.M. Tumir, M. Mlakar. *Electrochim. Acta* **2020**, 337, 135797.
13 8
14 9
15 [36] P. Cmuk, I. Piantanida, M. Mlakar. *Electroanalysis* **2009**, 21, 2527.
16 10
17 11
18 [37] V. Mirčeski, Š. Komorsky-Lovrić, M. Lovrić in Monography in Electrochemistry, (Ed. F.
19 12 Scholz) Springer-Verlag, Berlin **2009**, pp. 1625–1627.
20 13
21 14
22 [38] M. Mlakar. *Anal. Chim. Acta* **1993**, 276, 367–372.
23 15
24 16
25 [39] L. Čizmek, S. Komorsky-Lovrić, M. Lovrić. *Chem. Electro. Chem.* **2015**, 2, 2027–2031.
26 17
27 18
28 19
29 [40] B.M. Voelker, D. L. Sedlak, O. C. Zafiriou. *Environ. Sci. Technol.* **2000**, 34, 1036–1042.
30 20
31 21
32 [41] E.W. Bauman. *J. inorg. nucl. Chem.* **1974**, 36, 1827-1832.
33 22
34 23
35 [42] A. M. Cindrić, S. Marcinek, C. Garnier, P. Salaun, N. Cukrov, B. Oursel, V. Lenoble, D.
36 24 Omanović. *Total Environ.* **2020**, 721, 137784.
37 25
38 [43] H. Whitby, J. T. Hollibaugh, C. M. G. van den Berg. *Frontiers in Marine Science* **2017**, 4,
39 26 178–190.
40 27
41 28
42
43
44
45
46
47
48
49
50
51
52
53
54
55
56
57
58
59
60

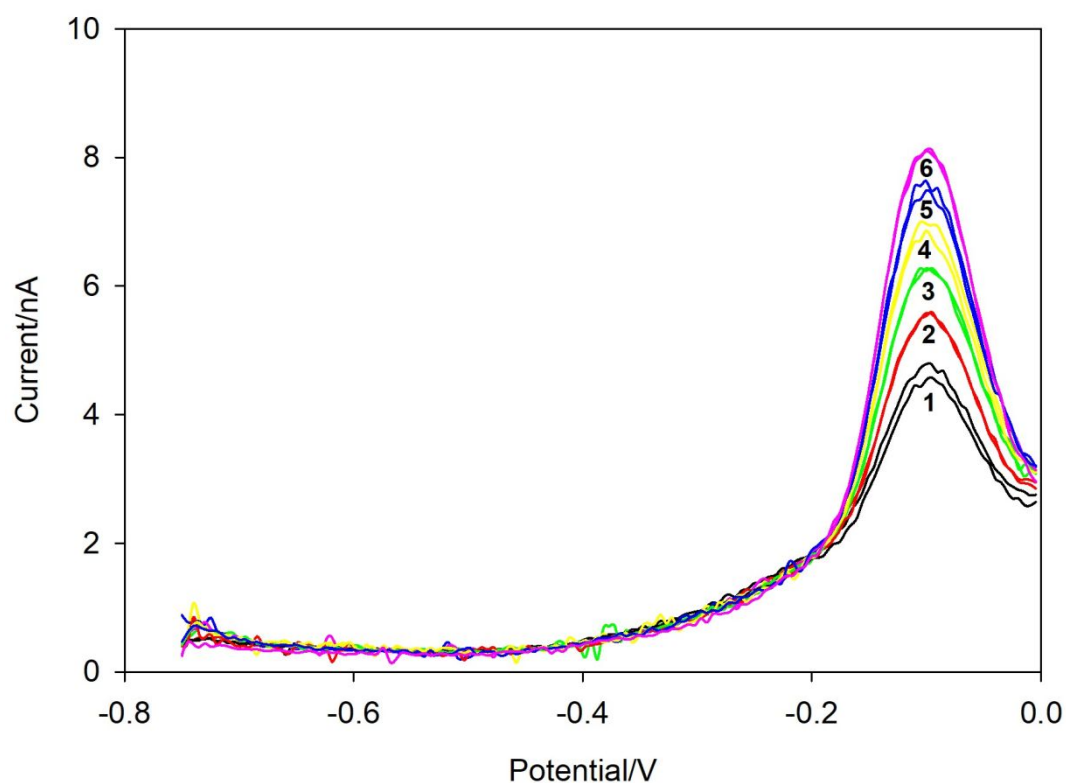


Figure 1S Determination of total dissolved Cu concentration using DP-ASV ($t_{acc}/s = 120$, $E_{acc} = -0.85$). Added Cu(II) as follows: 1 – 0, 2 – 1.9×10^{-8} , 3 – 3.9×10^{-8} , 4 – 5.8×10^{-8} , 5 – 7.7×10^{-8} , 6 – 9.6×10^{-8} . Next scanning parameters were used: step of 0.005 V, modulation time of 0.05 s, interval time of 0.5 s and modulation amplitude of 0.025 V and frequency 25 s^{-1} . The sample was diluted 2.5 times with acidified MQ water before the measurements.

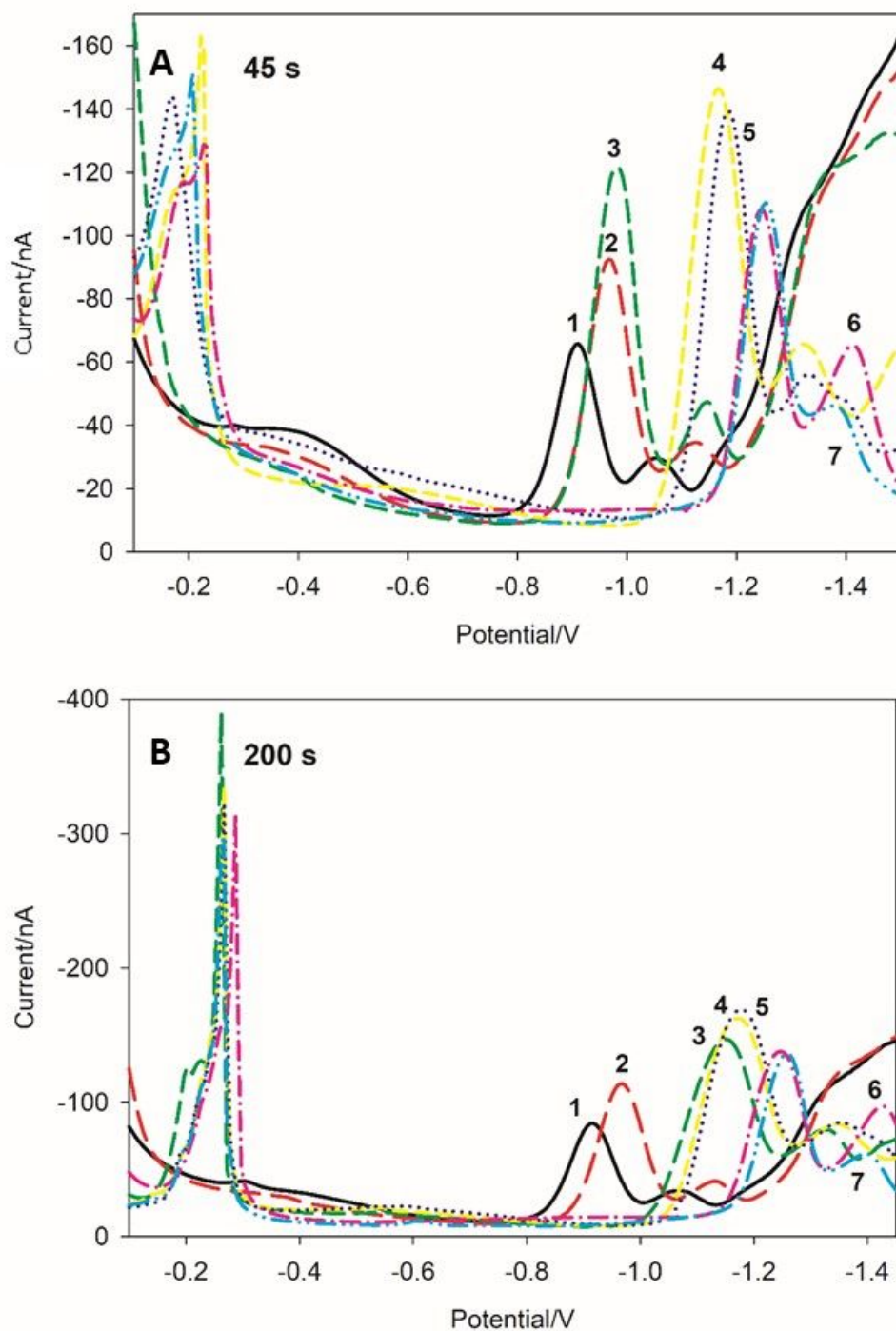


Figure 2S SWV of $6.6 \times 10^{-7} \text{ mol dm}^{-3}$ BCS in 0.55 mol dm^{-3} NaCl + 0.01 mol dm^{-3} borate buffer dependence on pH; $t_{\text{acc}}/s = 45 \text{ s}$ (A) and 200 s (B). pH: 1 – 2.5; 2 – 3.5; 3 – 4.5; 4 – 5.7; 5 – 6.7; 6 – 8.2; 7 – 9.0; deposition potential 0 V; A = 20 mV, f = 25 s.

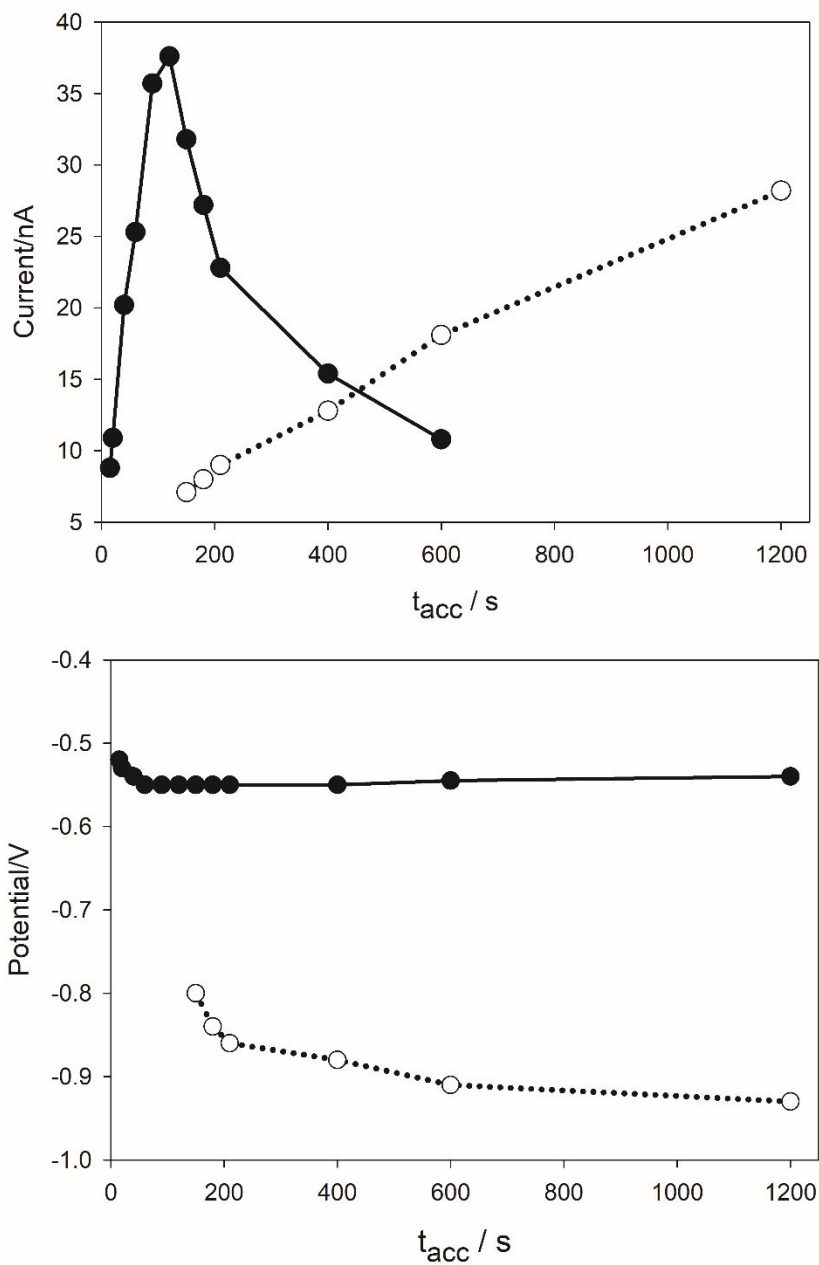


Figure 3S The peak currents and potentials dependence on the accumulation time for reduction of Cu(I)-BCS at about -0.55 V (●) and Cu(II)-BCS at around -0.90 V (○).

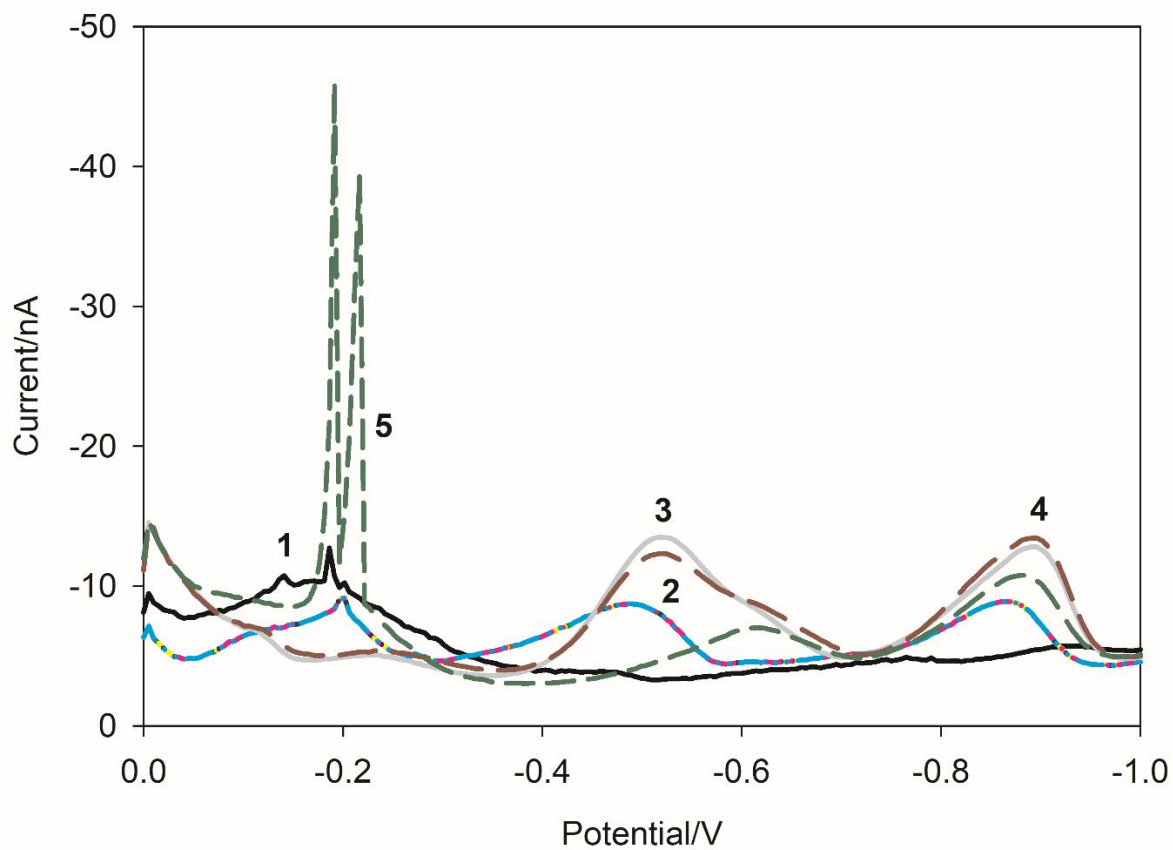


Figure 4S Copper titration with BCS in 0.55 M NaCl; pH = 8.2; $t_{\text{acc}} = 200$ s, $E_{\text{acc}} = 0.0$ V, $A = 20$ mV, $f = 25$ s^{-1} , $[\text{Cu}] = 4.2 \times 10^{-7}$ mol dm^{-3} ; $[\text{BCS}]/\text{mol dm}^{-3}$: 1 – 0; 2 – 2.1×10^{-7} ; 3 – 4.2×10^{-7} ; 4 – 6.4×10^{-7} ; 5 – 1.3×10^{-6} .

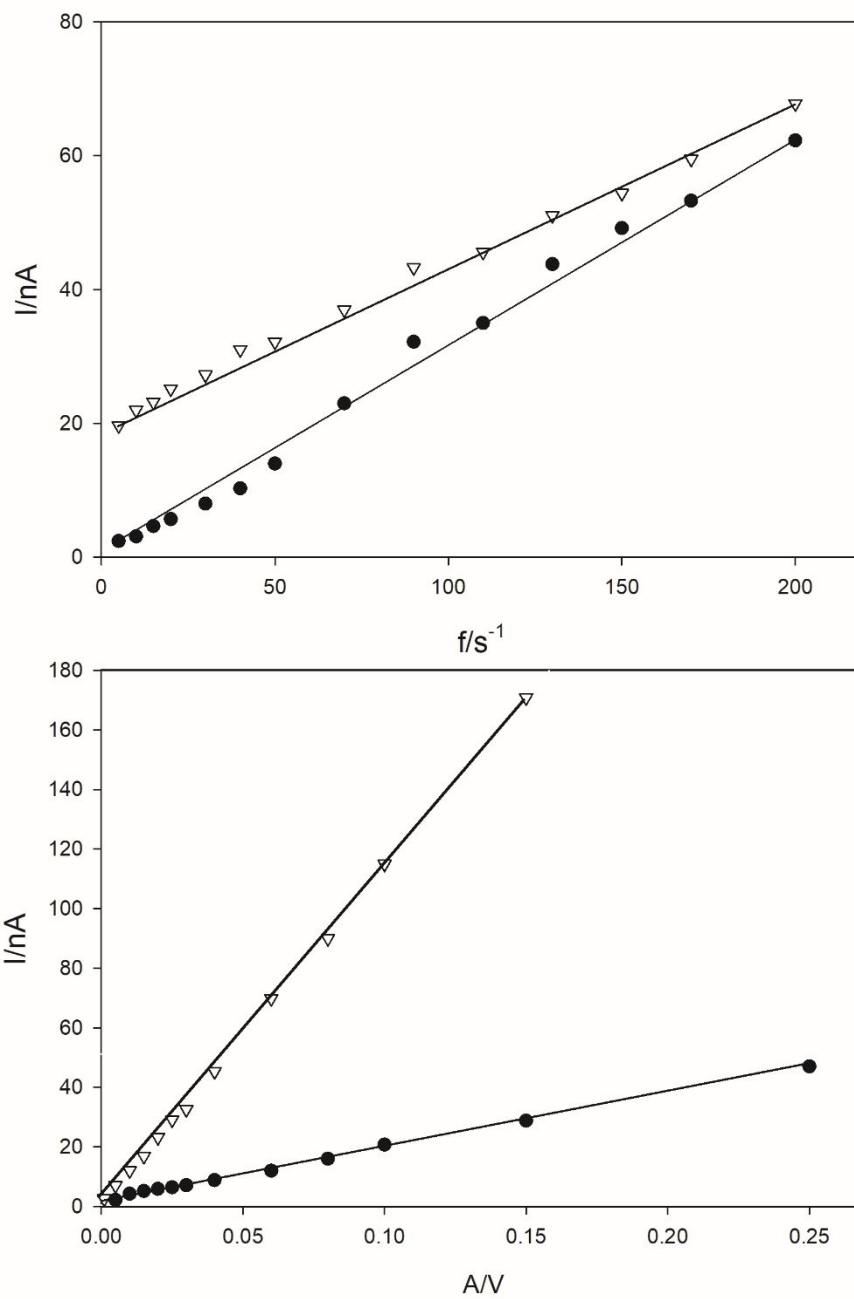


Figure 5S Dependence of Cu(I)-BCS reduction peak current at -0.55 V (∇), at -0.90 V (\bullet), on SW frequency and amplitude (pH 8.2, $t_{acc} = 200$ s, $E_{acc} = 0.0$ V).

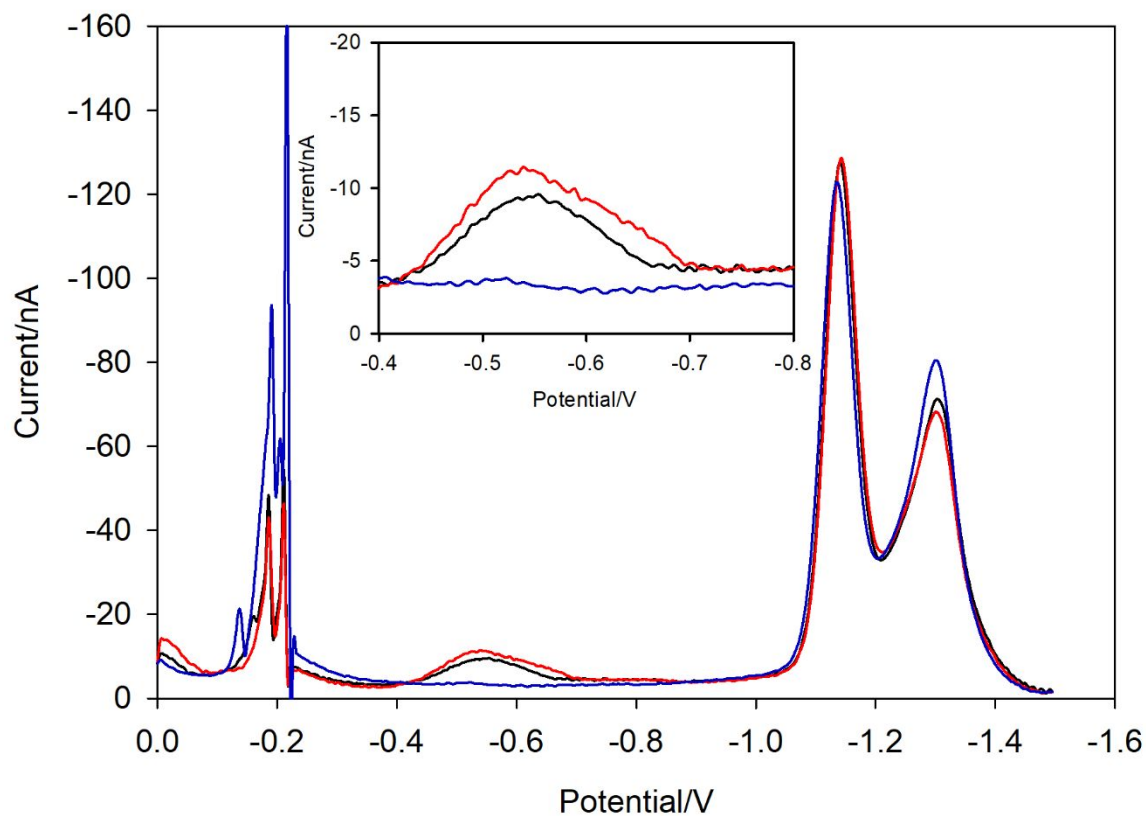


Figure 6S SWV at pH = 8.2; $t_{\text{acc}} = 120$ s, $E_{\text{acc}} = 0.0$ V, $A = 20$ mV, $f = 25$ s $^{-1}$. Red line - [Cu (I)] = 4.2×10^{-7} mol dm $^{-3}$; [BCS/EDTA] = 0.66×10^{-7} mol dm $^{-3}$ and 3.33×10^{-6} mol dm $^{-3}$, respectively. Black line - [Cu(I)] = 4.2×10^{-7} mol dm $^{-3}$ and BCS = 0.66×10^{-7} . Blue line - [Cu (II)] = 4.2×10^{-7} mol dm $^{-3}$; [BCS/EDTA] = 0.66×10^{-7} mol dm $^{-3}$ and 3.33×10^{-6} mol dm $^{-3}$, respectively. Supporting electrolyte = 0.55 mol dm $^{-3}$ NaCl + 0.01 mol dm $^{-3}$ borate buffer. Inset: Enlarged potential range from -0.4 to -0.8.

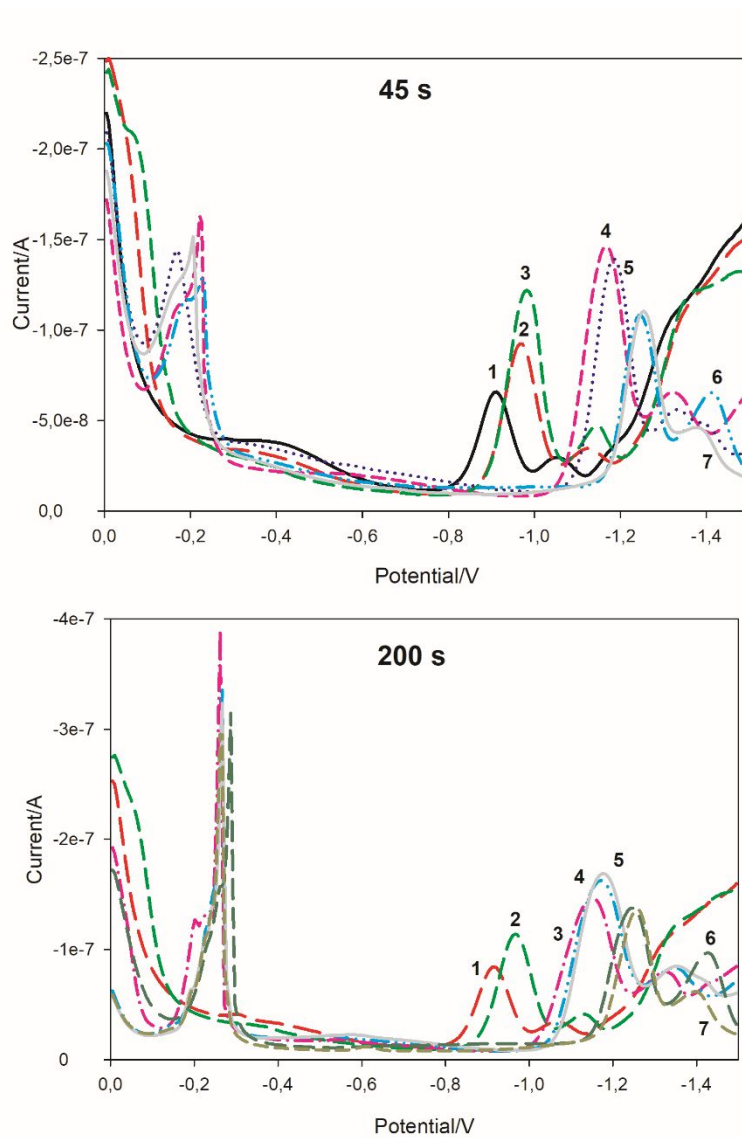


Figure 1S SWV of $6.6 \times 10^{-7} \text{ mol dm}^{-3}$ BCS in 0.55 mol dm^{-3} NaCl + 0.01 mol dm^{-3} borate buffer dependence on pH; $t_{\text{acc}}/s = 45 \text{ s}$ (A) and 200 s (B). pH: 1 – 2.5; 2 – 3.5; 3 – 4.5; 4 – 5.7; 5 – 6.7; 6 – 8.2; 7 – 9.0; deposition potential 0 V; $A = 20 \text{ mV}$, $f = 25 \text{ s}$.

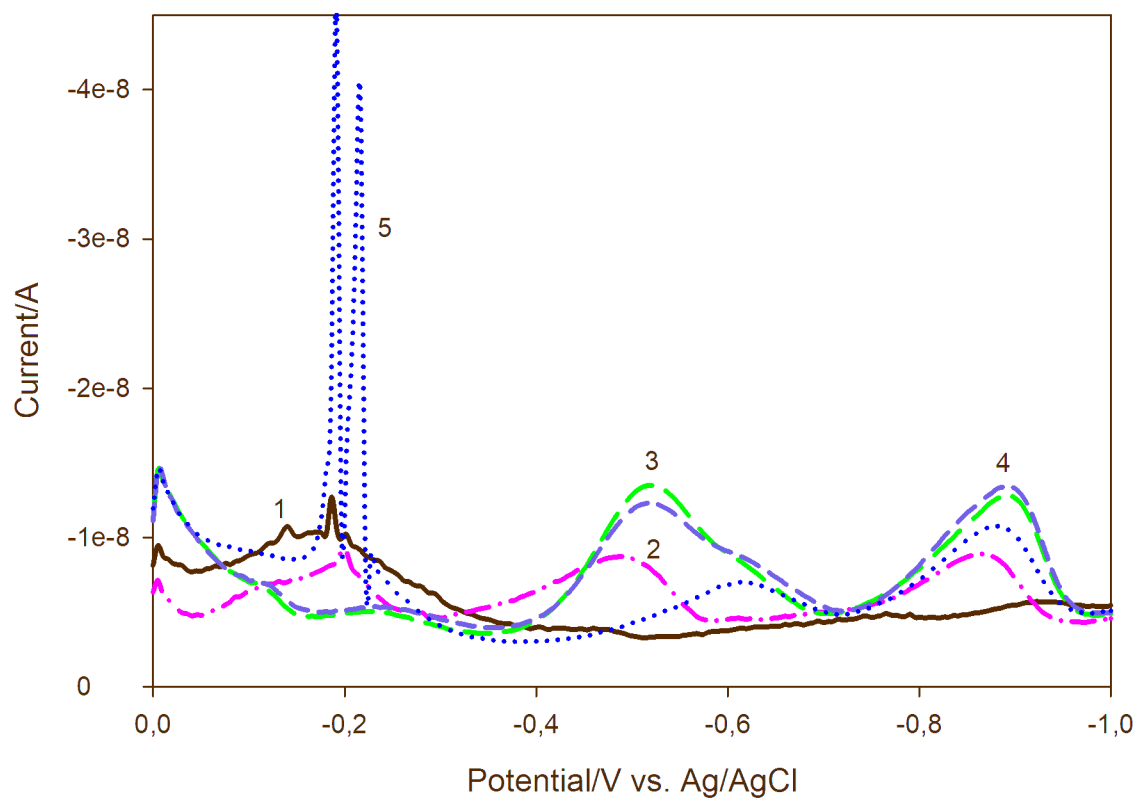


Figure 2S Copper titration with BCS in 0.55 M NaCl; pH = 8.2; $t_{acc} = 200$ s, $E_{acc} = 0.0$ V, $A = 20$ mV, $f = 25$ s $^{-1}$, $[Cu] = 4.2 \times 10^{-7}$ mol dm $^{-3}$; [BCS]/mol dm $^{-3}$: 1- 0; 2 - 2.1×10^{-7} ; 3 - 4.2×10^{-7} ; 4 - 6.4×10^{-7} ; 5 - 1.3×10^{-6} .